ELSEVIER

On the stability of oceanic vortices: A solution to the problem?

E.S. Benilov

Department of Mathematics, University of Limerick, Limerick, Ireland

Abstract

This paper attempts to resolve the long-standing contradiction between the observed longevity of oceanic vortices and their theoretical instability. Using the model of quasigeostrophic, two-layer ocean, we show that a vortex in the upper layer can be stabilised by a circulation in the lower layer, such that the potential vorticity (PV) there is uniform. It is also argued that the assumption of uniform PV in the 'passive' layer corresponds to the fact that most oceanic vortices are shed by frontal currents and are alien to the well-mixed water masses around them.
© 2005 Elsevier B.V. All rights reserved.

Keywords: Oceanic vortices; Potential vorticity; Stability

1. Introduction

1.1. Previous work

The contradiction between experimental and theoretical estimates of the lifespan of mesoscale oceanic vortices (rings) has been identified more than 20 years ago. Observations (e.g. Lai and Richardson, 1977) suggest that rings exist for years, whereas almost all theoretical works indicate that they are unstable. The first theoretical paper on the subject (Ikeda, 1981) examined quasigeostrophic vortices in a two-layer ocean and demonstrated that, for realistic oceanic parameters, rings with Gaussian deviation of the interface are un-

stable (see also, Carton and McWilliams, 1989, 1996). Several papers (Sokolovskiy, 1988, 1997; Helfrich and Send, 1988; Flierl, 1988) examined quasigeostrophic vortices in a two-/three-layer ocean – with potential vorticity of the vortex vanishing outside a circle – and arrived at similar conclusions. A more general conclusion has been obtained by Killworth et al. (1997) and Benilov et al. (1998) for two-layer and continuously stratified ocean, respectively: they showed that all vortices, the radii of which are much larger than the Rossby radius, are unstable regardless of their profiles.

Only two theoretical papers have found examples of stable rings.

The first such finding has been made by Paldor and Nof (1990). They considered ageostrophic, solid-body rotating vortex surrounded by a heavier fluid, and demonstrated that it is stable if sufficiently thin (thinner than, approximately, a one-quarter of the total depth of the ocean). This result would resolve the paradox, as most oceanic rings are indeed thin. However, Benilov (2003) showed that instability of thin vortices is generally caused by critical layers. Unfortunately, this devalued the result of Paldor and Nof (1990), as solid-body rotating vortex does not have critical layers and, as such, is not a good model for (differentially rotating) oceanic rings.

Another mechanism of ring stabilization has been suggested by Dewar and Killworth (1995), who considered a Gaussian vortex in the upper layer of a two-layer ageostrophic ocean and a relatively weak co-rotating circulation in the lower layer ('deep flow'). It turned out that the latter can stabilize the ring, or at least considerably reduce the growth rate of instability. This result has been later extended to other vortex shapes by Katsman et al. (2003) and, in all examples considered, a co-rotating deep flow reduced the growth rate; however, no profile other than the Gaussian one would become completely stable.

1.2. A new approach

Before we describe the results of the present work, note that Dewar and Killworth (1995) and Katsman et al. (2003) assumed that the deep circulation has the same profile as the upper-layer vortex. A different approach has been used by Benilov (2004): the profile of the deep flow will be derived from the assumption that potential vorticity (PV) in the lower layer is constant. Such model is suggested by the fact that most oceanic vortices are shed by unstable frontal currents: when a vortex moves away from the current and arrives to a new location, the PV field below it cannot change and must remain equal to its initial, background value. Observe also that the interface displacement, caused by the vortex, contributes to the lower-layer PV; hence, to maintain its initial value, the lower-layer spins up. Remarkably, the resulting circulation is always co-rotating, and never counter-rotating!

In order to understand how the deep circulation with uniform PV affects the vortex, observe that normally vortices are unstable due to the interaction of two phase-locked disturbances propagating 'around' the vortex in the upper and lower layers. These disturbances are, essentially, Rossby waves, as they are supported by the gradient of the vortex's PV field. Accordingly, the uniform PV-field in the lower layer eliminates one of the disturbances and makes the vortex baroclinically stable. As for the barotropic instability, it was shown to require strong horizontal shear (Benilov, 2003), such that never occurs in mesoscale rings. Thus, mesoscale vortices with uniform PV in the lower layer appear to be both baroclinically and barotropically stable.

The present contribution presents a brief summary of the paper by Benilov (2004), adapting it for physics-minded readers. We shall demonstrate the stability of vortices with uniform PV in the lower layer, in a two-layer ocean with thin upper layer, using the (simplest) quasigeostrophic model. In Section 2, we shall formulate the linearized equations for harmonic disturbances (normal modes) superposed on the vortex. In Section 3, through numerical solution of the eigenvalue problem, we shall present several examples of stable vortices with different profiles in the upper layer and uniform PV in the lower layer. In Section 4, we shall derive an asymptotic stability criterion for thin vortices with a weak deep flow and show that it is satisfied for vortices with uniform lower-layer PV.

2. Governing equations

Consider a two-layer ocean with rigid lid and flat bottom, and let the densities and depths of the layers be $\rho_{1,2}$ and $H_{1,2}$ (where subscript 1 marks the upper layer). We shall also introduce the upper-layer Rossby (deformation) radius:

$$L_d = \frac{\sqrt{g'H_1}}{f_0},$$

where $g' = g(\rho_2 - \rho_1)/\rho_2$ is the reduced gravity and f_0 is the Coriolis parameter. Using L_d and the characteristic velocity V_{*1} of the flow in the upper layer, we shall introduce the following non-dimensional variables:

$$t = \frac{V_{*1}t_*}{L_d}, \qquad r = \frac{r_*}{L_d}, \qquad \theta = \theta_*, \qquad \psi_{1,2} = \frac{\psi_{*1,2}}{L_d V_{*1}},$$

where t is the time, (r, θ) the polar coordinates, $\psi_{1,2}$ the streamfunctions, and asterisks mark the dimensional variables.

We are concerned with linear stability of radially symmetric vortices, and assume:

$$\psi_{1,2} = \Psi_{1,2}(r) + \psi'_{1,2}(r, \theta, t),$$

where $\Psi_{1,2}$ describes the vortex, and $\psi_{1,2}$, the disturbance. We shall seek normal modes, i.e. solutions of the form:

$$\psi'_{1,2}(r, \theta, t) = \text{Re}[\phi_{1,2}(r)\, e^{ik(\theta - ct)}],$$

where k and c are the azimuthal wavenumber and angular phase speed, respectively.

For description of vortices, we shall employ the linearized quasigeostrophic equations on the f-plane (for more details, see Benilov, 2003),

$$(cr - V_1)\left[\frac{1}{r}\frac{d}{dr}\left(r\frac{d\phi_1}{dr}\right) - \frac{k^2}{r^2}\phi_1 - \phi_1 + \phi_2\right] + Q'_1\phi_1 = 0, \tag{1}$$

$$(cr - V_2)\left[\frac{1}{r}\frac{d}{dr}\left(r\frac{d\phi_2}{dr}\right) - \frac{k^2}{r^2}\phi_2 - \varepsilon\phi_2 + \varepsilon\phi_1\right] + Q'_2\phi_2 = 0, \tag{2}$$

where

$$\varepsilon = \frac{H_1}{H_2}$$

is the depth ratio,

$$V_{1,2} = \frac{d\Psi_{1,2}}{dr}$$

are the swirl velocities in the layers, and

$$Q_1' = \frac{d}{dr}\left[\frac{1}{r}\frac{d}{dr}(rV_1)\right] - V_1 + V_2, \qquad Q_2' = \frac{d}{dr}\left[\frac{1}{r}\frac{d}{dr}(rV_2)\right] - \varepsilon V_2 + \varepsilon V_1$$

are the corresponding PV gradients.

Equations (1) and (2) should be supplemented by the usual boundary conditions,

$$\phi_{1,2}(0) = \phi_{1,2}(\infty) = 0. \tag{3}$$

(1)–(3) form a boundary-value problem, where c is the eigenvalue. If Im $c > 0$, the vortex is unstable.

In what follows, we shall assume that $V_1(r)$ and $V_2(r)$ are smooth functions, decaying as $r \to \infty$ and vanishing at $r = 0$ (the latter condition guarantees that the vortex is smooth at its centre). We shall also assume that

$$0 < \int_0^\infty r^2 V_1 \, dr < \infty, \tag{4}$$

i.e. the upper-layer net angular momentum of the vortex is finite and non-zero.

3. Numerical results

In this section, problems (1)–(3) will be solved numerically. Firstly, we shall briefly discuss compensated vortices, i.e. those that have no flow in the lower layer. Secondly, we shall examine several examples of vortices with uniform PV in the lower layer.

3.1. Compensated vortices

In this case, the lower layer is at rest,

$$V_2 = 0, \tag{5}$$

and we consider the following three examples of vortices in the upper layer:

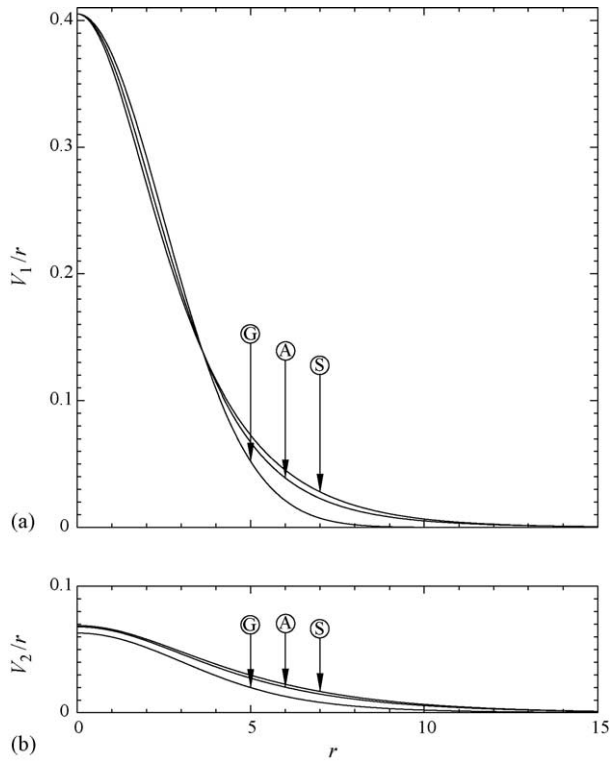$$V_{1G} = \frac{r}{r_0} \exp\left(-\frac{r^2}{2r_0^2}\right), \tag{6}$$

Fig. 1. Profiles of angular velocity for vortices considered in the paper. In the upper layer, the vortex is determined by (6), or (7), or (8) (the Gaussian, or Algebraic, or Sech profiles, marked by G, A, and S, respectively)—see panel (a). In the lower layer, the profile of the vortex is either $V_2 = 0$ (compensated vortices), or defined by equations (11) and (12) (vortices with uniform PV in the lower layer). The latter type is shown on panel (b).

$$V_{1A} = \frac{r}{r_0} \left(1 + \frac{r^2}{5r_0^2} \right)^{-3}, \tag{7}$$

$$V_{1S} = \frac{r}{r_0} \operatorname{sech} \left(\frac{1.186r}{r_0} \right), \tag{8}$$

where r_0 is the non-dimensional radius of the vortex (i.e. the ratio of its dimensional radius to the deformation radius based on the upper-layer depth). The coefficients in these expressions have been chosen to ensure that the maximum of $V_1(r)$ is located at $r = r_0$ (for (8), this equality is approximate, $r \approx r_0$). Profiles (6)–(8) will be referred to as the Gaussian, Algebraic, and Sech vortices, respectively. The corresponding profiles of the upper-layer angular velocity, V_1/r, are shown in Fig. 1a—to a naked eye, the three profiles are not all that different.

The stability of the Gaussian, Algebraic, and Sech vortices was explored by Benilov (2003) in a wide range of parameters, both asymptotically and numerically (hereinafter, this work will be referred to as B03). It was demonstrated that the most unstable azimuthal

wavenumber is either $k = 1$ or 2. It was also shown that, for a given k, the Gaussian vortex admits a finite number of eigenvalues. The first eigenvalue[1] always has the highest growth rate. Moreover, when parameters of a stable Gaussian vortex change, the first eigenvalue becomes unstable before the others, which makes it a 'stability indicator'. The Sech vortex, in turn, may have either finite or infinite number of eigenvalues (depending on whether $r_0 < 1.186$ or 1.186), but the first mode is, again, the stability indicator. Finally, the Algebraic vortex admits infinitely many eigenvalues for each k, and the first eigenvalue loses stability *after* all the others—although, in many cases, it is still the most unstable one (when, of course, it *is* unstable).

The most important characteristic of a vortex profile is the corresponding marginal stability curve on the (ε, r_0)-plane. It was computed for the three types of compensated vortices, for the first eigenvalue of the second azimuthal wavenumber, $k = 2$. As $\varepsilon \to 0$ (the limit of infinitely thin upper layer), the solution of the eigenvalue problems (1)–(3) is increasingly difficult to compute, and we complemented the numerical solution by an asymptotic one, obtained via a method developed in B03.

The results are shown in Fig. 2.

Observe that the Gaussian profile has two regions of instability (see Fig. 2a). The narrow strip with small r_0 corresponds to *barotropic* instability, caused by strong *horizontal* shear, whereas vortices with large r_0 are unstable *baroclinically* due to *vertical* shear. Note also that, if the two types of shear are comparable, they, in a sense, cancel each other, which explains the region of stability in the middle area of Fig. 2a [this effect has been previously noted by Dewar and Killworth (1995)]. Observe also that the Algebraic and Sech profiles are barotropically stable.

To place the above results in oceanographic context, Fig. 2 shows the parameters of the 35 rings catalogued by Olson (1991) (this paper will be referred to as O91). Unfortunately, O91 provides no data on the depth ratio ε, and we have to assume, on a more or less ad hoc basis, that

$$0.05 \le \varepsilon \le 0.1.$$

Thus, each ring in Fig. 2 is represented by an interval with a fixed r_0, but uncertain ε. One can see that the Algebraic model (Fig. 2b) predicts that all rings are unstable for all possible ε, and the predictions of the Sech model are similar. The Gaussian model is the only one producing rings which are stable for the whole ε range (these are the six rings with the smallest values of r_0). Overall, the proportion of stable vortices is far too low to account for oceanic observations.

Still, one might argue that the instability is so weak that unstable rings survive for a long time before breaking up, which would explain the lifespans observed. To eliminate this possibility, we have computed the growth rate for the Gaussian vortex of radius 65 km (which is the average over the rings listed in O91), in the ocean with deformation radius of 27 km (which is, again, an average derived from O91). Non-dimensionally, these values correspond to:

---

[1] Here, the eigenvalues are enumerated according to the number of nodes of the lower-layer eigenfunction: the first eigenfunction has no nodes, the second one has one node, etc.
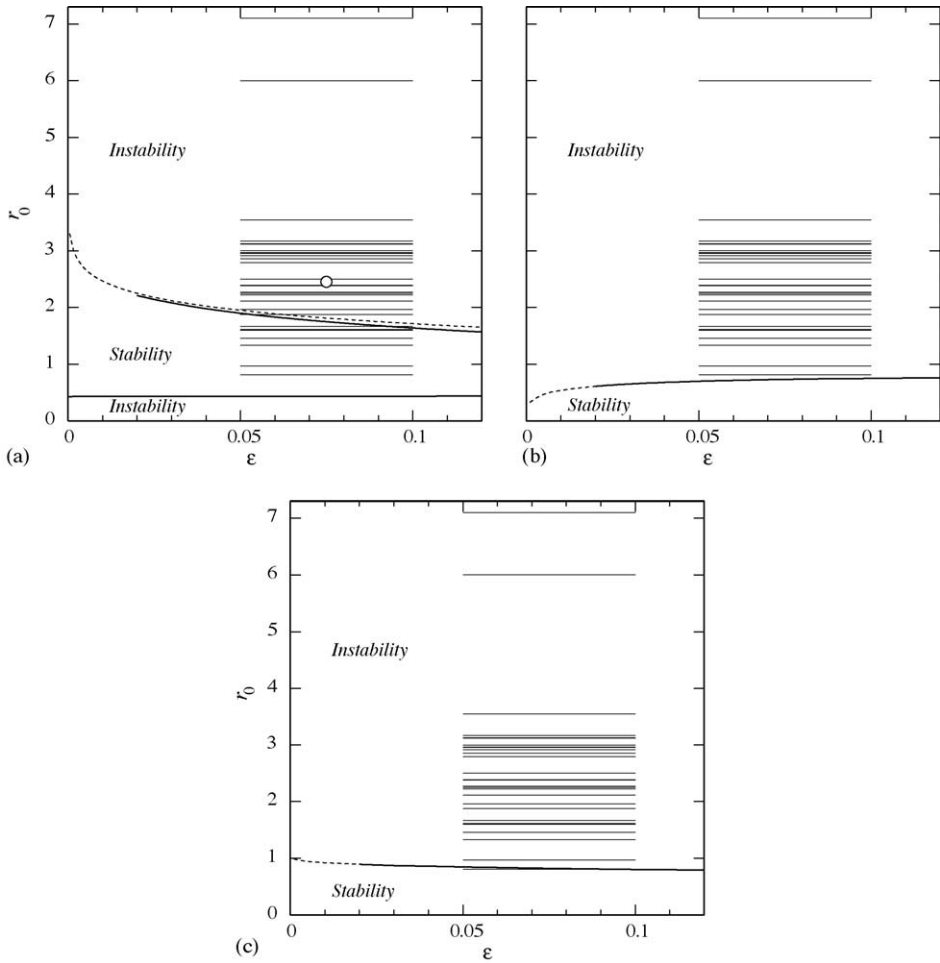
Fig. 2. Stability of compensated vortices with respect to the first mode of $k = 2$, on the (ε, r_0)-plane (ε is the depth ratio of the ocean, r_0 is the non-dimensional radius of the vortex). Solid line shows the numerical results, dotted line shows the asymptotic results (based on $\varepsilon \ll 1$); horizontal segments show the parameters of rings catalogued by Olson (1991). (a) Gaussian vortex (6), (b) Algebraic vortex (7), (c) Sech vortex (8). The circle in the centre of (a) shows the 'mean' vortex (9) and (10).

$$r_0 = 2.47. \tag{9}$$

With regard to ε, we shall assume the mid point of this parameter's range:

$$\varepsilon = 0.075 \tag{10}$$

(Values (9) and (10) are shown in Fig. 2a by a circle.) In this case, the first eigenvalue with $k = 2$ is the most unstable one, with a growth rate of $k \, \mathrm{Im} \, \omega \approx 0.01711$. To put this into dimensional terms, we need to fix the ring's maximum swirl velocity. Unfortunately, O91

provides only the 'absolute' maximum of the swirl velocity, whereas we need the maximum of the swirl velocity averaged over the upper layer's depth, $V_{*1\,\text{max}}$ (which is a restriction imposed by the two-layer model). Estimating $V_{*1\,\text{max}}$ to be within the range of 0.1–0.25 m/s, we obtain the e-folding time of 111–44 days, respectively. Clearly, this is much shorter than the lifespans of most oceanic rings.

Thus, the model of compensated vortices cannot explain the observed longevity of rings.

3.2. Vortices with uniform PV in the lower layer

For the upper-layer velocity, we considered the same three examples as before, (6)–(8). The lower-layer velocity, in turn, was assumed to satisfy the condition that the PV gradient is zero,

$$\frac{\text{d}}{\text{d}r}\left[\frac{1}{r}\frac{\text{d}}{\text{d}r}(rV_2)\right] - \varepsilon V_2 + \varepsilon V_1 = 0, \tag{11}$$

and the usual boundary conditions:

$$V_2(0) = V_2(\infty) = 0. \tag{12}$$

As an illustration, Fig. 1b shows the solution of the boundary-value problems (11) and (12) for the Gaussian, Algebraic, and Sech vortices, with the 'mean' parameters (9) and (10).

It turned out that vortices with an Algebraic or Sech profile in the upper layer, and uniform PV in the lower layer, are stable for all values of ε and r_0—a thorough search failed to find a single unstable vortex. For the Gaussian profile in the upper layer (and, again, uniform PV in the lower one), the region of barotropically unstable vortices looks almost the same as that for compensated vortices, but the region of baroclinically unstable vortices disappears completely. Thus, the model of uniform PV in the lower layer predicts that all rings listed in O91 are stable.

To illustrate the transition from compensated vortices to those with uniform PV in the lower layer, consider:

$$V_2 = \alpha(V_2)_{\text{uPV}}, \tag{13}$$

where $(V_2)_{\text{uPV}}$ is the solution of the uniform-PV problems (11) and (12), and α is a number between 0 (compensated vortex) and 1 (uniform PV in the lower layer). A large number of vortices, with various parameters, were tested for stability, and in all cases the growth rate vanished for some $\alpha < 1$. A typical behavior of the non-dimensional growth rate is shown in Fig. 3 for the 'mean' vortex (9) and (10): one can see that, for all three upper-layer profiles, the vortex becomes stable at $\alpha \approx 0.65$. It is also worth observing that, for $0.45 \leq \alpha \leq 0.65$, the three curves virtually coincide.

We have also computed the marginal stability curves for $\alpha = 0.65$ (for the details of the numerical technique, see Benilov, 2004). For the Algebraic and Sech upper-layer profiles, these curves are very close, and we show only the one corresponding to the former (see Fig. 4b). The Gaussian profile is different (see Fig. 4a), but only as far as barotropic instability
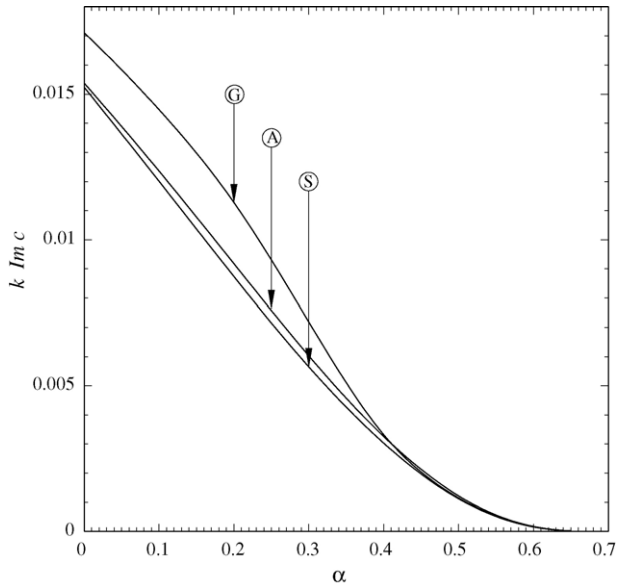
Fig. 3. The growth rate of the first mode of $k = 2$, for the 'mean' vortex ($\varepsilon = 0.075$, $r_0 = 2.47$), vs. the amplitude α of the lower-layer circulation. The lower-layer velocity is determined by (13) (where $\alpha = 0$ corresponds to compensated vortices, and $\alpha = 1$ corresponds to vortices with uniform PV in the lower layer); 'G', 'A', and 'S' mark the Gaussian, Algebraic, and Sech vortex profiles.
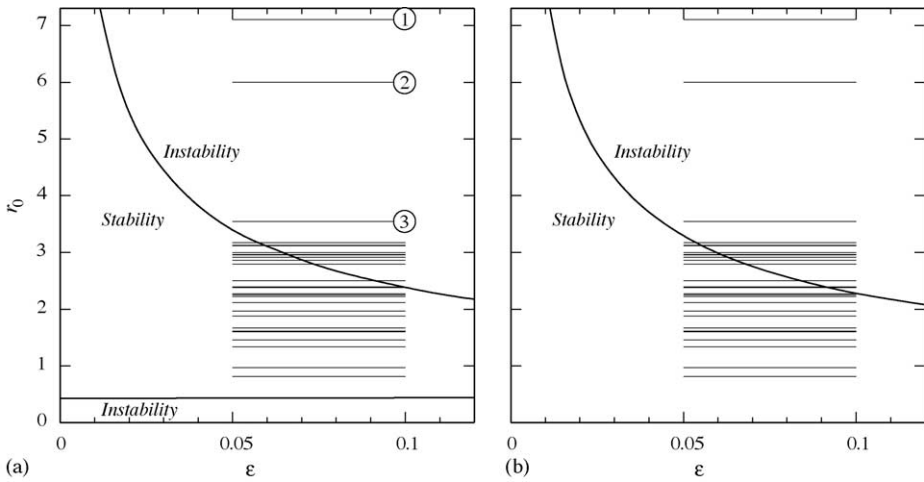

Fig. 4. Stability of non-compensated vortices with respect to the first mode of $k = 2$. In the upper layer, the vortex is determined by (6), (7), or (8), and the lower-layer circulation determined by (13) with $\alpha = 0.65$. The notation is the same as in Fig. 2. (a) Gaussian vortex [the circles mark vortices with parameters (14) and (15)] and (b) Algebraic vortex.

is concerned, whereas the curve separating baroclinically unstable vortices from the stable ones is almost the same as that in the other two cases.

One can see that, for non-compensated vortices determined by (13) with $\alpha = 0.65$, the stability region has noticeably expanded (compare Fig. 4a and b to Fig. 2a and b). Moreover, the growth rate of vortices that are still unstable has fallen dramatically! Indeed, consider the three rings on the O91 list that have the largest values of r_0,

$$r_0 = 7.105, \ 6.000, \ 3.548 \tag{14}$$

(In Fig. 4a, these values are marked by circles with numbers 1–3, respectively.) The corresponding values of the deformation radius, extracted from O91, are:

$$L_d = 42, \ 10, \ 19 \, (\text{km}).$$

We shall assume that

$$\varepsilon = 0.1, \tag{15}$$

which is the most unstable value of the ε range considered before. Finally, we put

$$V_{*1 \, max} = 0.25 \, (\text{m/s}),$$

which is, again, the most unstable value of the range considered. For rings with these parameters, with Gaussian profile in the upper layer and profile (13) ($\alpha = 0.65$) in the lower layer, the (dimensional) e-folding times are 6.6 months, 8.9 months, and 14.4 years, respectively.

Thus, one of the rings is virtually stable, whereas the lifespan of the other two is sufficiently large to fit with, at least, some observations.

We note that the case $\alpha < 1$ can be viewed as a simple model of a non-uniformity of PV in the lower layer, including those that are caused by background currents (which are often present in the 'real' ocean). The existence of stable vortices with $\alpha < 1$ demonstrates the robustness of the suggested mechanism of stabilization and shows that stability persists in the face of less than ideal conditions.

Finally, note that flow (13) is not the only possibility to stabilize the vortex—after all, Dewar and Killworth (1995) did show that, for Gaussian vortices, a co-rotating Gaussian circulation has the same effect. Our point is that (13) stabilizes all vortices regardless of their profiles, and also appears to be a realistic model of oceanic rings.

4. Asymptotic results

Assume that the upper layer is much thinner than the lower layer,

$$\varepsilon \ll 1,$$

and that the flow in the latter is weak, say, $V_2 = \mathrm{O}(\varepsilon)$ (it may or may not correspond to uniform PV, as we shall first consider the general case). Accordingly,

$$V_2 = \varepsilon \tilde{V}_2,$$

where $\tilde{V}_2 = O(1)$. Rewriting equations (1) and (2) in terms of $\tilde{V}_2$ and omitting the tildes, we obtain:

$$
(cr - V_1)\left[\frac{1}{r}\frac{d}{dr}\left(r\frac{d\phi_1}{dr}\right) - \frac{k^2}{r^2}\phi_1 - \phi_1 + \phi_2\right]
$$
$$
+ \left\{\frac{d}{dr}\left[\frac{1}{r}\frac{d}{dr}(rV_1)\right] - V_1 + \varepsilon V_2\right\}\phi_1 = 0, \tag{16}
$$

$$
(cr - \varepsilon V_2)\left[\frac{1}{r}\frac{d}{dr}\left(r\frac{d\phi_2}{dr}\right) - \frac{k^2}{r^2}\phi_2 - \varepsilon\phi_2 + \varepsilon\phi_1\right]
$$
$$
+ \varepsilon\left\{\frac{d}{dr}\left[\frac{1}{r}\frac{d}{dr}(rV_2)\right] - \varepsilon V_2 + V_1\right\}\phi_2 = 0. \tag{17}
$$

Observe that the eigenvalue problems (16) and (17), (3) is satisfied by:

$$
c = 0, \qquad \phi_1 = V_1, \qquad \phi_2 = \varepsilon V_2 \quad \text{for} \quad k = 1. \tag{18}
$$

(18) corresponds to an infinitesimal shift of the vortex as a whole and has nothing to do with its stability—it will be referred to as the *trivial solution*.

4.1. The classification of modes

Seek a solution in the form:

$$
\phi_1 = \phi_1^{(0)} + \varepsilon\phi_1^{(1)} + \cdots, \qquad \phi_2 = \phi_2^{(0)} + \varepsilon\phi_2^{(1)} + \cdots, \qquad c = c^{(0)} + \varepsilon c^{(1)} + \cdots,
$$

To the leading order, the eigenvalue problems (16) and (17), (3) yields:

$$
(c^{(0)}r - V_1)\left[\frac{1}{r}\frac{d}{dr}\left(r\frac{d\phi_1^{(0)}}{dr}\right) - \frac{k^2}{r^2}\phi_1^{(0)} - \phi_1^{(0)} + \phi_2^{(0)}\right]
$$
$$
+ \left\{\frac{d}{dr}\left[\frac{1}{r}\frac{d}{dr}(rV_1)\right] - V_1\right\}\phi_1^{(0)} = 0,
$$
$$
\phi_1^{(0)}(0) = \phi_1^{(0)}(\infty) = 0.
$$

$$
c^{(0)}r\left[\frac{1}{r}\frac{d}{dr}\left(r\frac{d\phi_2^{(0)}}{dr}\right) - \frac{k^2}{r^2}\phi_2^{(0)}\right] = 0, \tag{19}
$$

$$
\phi_2^{(0)} = 0, \qquad \phi_2^{(0)}(\infty) = 0. \tag{20}
$$

It follows from (19) and (20) that either $c^{(0)} = 0$, or $\phi_2^{(0)} = 0$, or both. Accordingly, we shall distinguish three types of modes.

(1) If

$$\phi_2^{(0)} = 0, \quad c^{(0)} \neq 0,$$

the upper-layer problem, to leading order, decouples from its lower-layer counterpart,

$$(c^{(0)}r - V_1)\left[\frac{1}{r}\frac{\mathrm{d}}{\mathrm{d}r}\left(r\frac{\mathrm{d}\phi_1^{(0)}}{\mathrm{d}r}\right) - \frac{k^2}{r^2}\phi_1^{(0)} - \phi_1^{(0)}\right]$$
$$+ \left\{\frac{\mathrm{d}}{\mathrm{d}r}\left[\frac{1}{r}\frac{\mathrm{d}}{\mathrm{d}r}(rV_1)\right] - V_1\right\}\phi_1^{(0)} = 0, \tag{21}$$

$$\phi_1^{(0)}(0) = \phi_1^{(0)}(\infty) = 0. \tag{22}$$

It describes the usual equivalent-barotropic motion, and its solutions will be referred to as *upper layer dominated (ULD) modes*.

(2) If

$$\phi_2^{(0)} = 0, \quad c^{(0)} \neq 0,$$

the lower-layer problem decouples from its upper-layer counterpart,

$$(c^{(1)}r - V_2)\left[\frac{1}{r}\frac{\mathrm{d}}{\mathrm{d}r}\left(r\frac{\mathrm{d}\phi_2^{(0)}}{\mathrm{d}r}\right) - \frac{k^2}{r^2}\phi_2^{(0)}\right] + \left\{\frac{\mathrm{d}}{\mathrm{d}r}\left[\frac{1}{r}\frac{\mathrm{d}}{\mathrm{d}r}(rV_2)\right] + V_1\right\}\phi_2^{(0)} = 0, \tag{23}$$

$$\phi_2^{(0)}(0) = \phi_2^{(0)}(\infty) = 0, \tag{24}$$

and determines the leading-order eigenvalue $c^{(1)}$. It describes oscillations in the lower layer, and its solutions will be referred to as *lower layer dominated (LLD) modes*.[2]

(3) If

$$\phi_2^{(0)} = 0, \quad c^{(0)} = 0,$$

the upper-layer problem becomes:

$$-V_1\left[\frac{1}{r}\frac{\mathrm{d}}{\mathrm{d}r}\left(r\frac{\mathrm{d}\phi_1^{(0)}}{\mathrm{d}r}\right) - \frac{k^2}{r^2}\phi_1^{(0)} - \phi_1^{(0)}\right] + \left\{\frac{\mathrm{d}}{\mathrm{d}r}\left[\frac{1}{r}\frac{\mathrm{d}}{\mathrm{d}r}(rV_1)\right] - V_1\right\}\phi_1^{(0)} = 0, \tag{25}$$

$$\phi_1^{(0)}(0) = \phi_1^{(0)}(\infty) = 0. \tag{26}$$

---

[2] Although ψ_1 and ψ_2, in this case, are of the same order, the larger thickness of the lower layer makes it dominant.

Observe that the eigenvalue $c^{(1)}$ does not appear in (25) and (26); thus, we shall need to examine the next order,

$$c^{(1)}r\left[\frac{1}{r}\frac{d}{dr}\left(r\frac{d\phi_1^{(0)}}{dr}\right) - \frac{k^2}{r^2}\phi_1^{(0)} - \phi_1^{(0)}\right]$$

$$+ V_1\left[\frac{1}{r}\frac{d}{dr}\left(r\frac{d\phi_1^{(1)}}{dr}\right) - \frac{k^2}{r^2}\phi_1^{(1)} - \phi_1^{(1)} + \phi_2^{(1)}\right]$$

$$+ \left\{\frac{d}{dr}\left[\frac{1}{r}\frac{d}{dr}(rV_1)\right] - V_1\right\}\phi_1^{(1)} + V_2\phi_1^{(0)} = 0, \tag{27}$$

$$\phi_1^{(1)}(0) = \phi_1^{(1)}(\infty) = 0. \tag{28}$$

$$c^{(1)}r\left[\frac{1}{r}\frac{d}{dr}\left(r\frac{d\phi_2^{(1)}}{dr}\right) - \frac{k^2}{r^2}\phi_2^{(1)} + \phi_1^{(0)}\right] + \left\{\frac{d}{dr}\left[\frac{1}{r}\frac{d}{dr}(rV_2)\right] + V_1\right\}\phi_2^{(1)} = 0, \tag{29}$$

$$\phi_2^{(1)}(0) = \phi_2^{(1)}(\infty) = 0, \tag{30}$$

Thus, $c^{(1)}$ depends on both eigenfunctions, and the corresponding solutions will be referred to as *mixed* (*M*) *modes*.

It turns out that the leading-order problems (25) and (26) have a solution only for the first azimuthal wavenumber, $k = 1$, in which case $\phi_1^{(0)} = V_1$ (see Appendix A). As a result, (29) becomes:

$$c^{(1)}r\left[\frac{1}{r}\frac{d}{dr}\left(r\frac{d\phi_2^{(1)}}{dr}\right) - \frac{1}{r^2}\phi_2^{(1)} + V_1\right] + \left\{\frac{d}{dr}\left[\frac{1}{r}\frac{d}{dr}(rV_2)\right] + V_1\right\}\phi_2^{(1)} = 0. \tag{31}$$

It can also be shown (again, see Appendix A) that $\phi_1^{(1)}$ can be eliminated form the first-order upper-layer problems (27) and (28), which can be reduced then to:

$$\int_0^\infty rV_1(c^{(1)}r - V_2)\,dr + \int_0^\infty rV_1\phi_2^{(1)}\,dr = 0. \tag{32}$$

Equations (30) and (32) form a closed eigenvalue problem for $\phi_2^{(1)}$ and $c^{(1)}$.

4.2. Summary

Thus, the exact eigenvalue problems (16) and (17), (3) has been reduced to three asymptotic (leading-order) problems.

- If the asymptotic problem for ULD-modes, (21) and (22), has one or more complex eigenvalues, the vortex is unstable, and the growth rate is $k \operatorname{Im} c = O(1)$.
- If the asymptotic problems for LLD- and M-modes [(23) and (24), and (30) and (32), respectively] have one or more complex eigenvalues, the vortex is unstable with a relatively small growth rate, $k \operatorname{Im} c = O(\varepsilon)$.
- If the three problems have some non-trivial ($c \neq 0$) real eigenvalues, but no complex ones, no definitive conclusion can be drawn. The vortex can be either stable, or weakly unstable due to the higher-order corrections.[3]
- If the three problems have neither complex nor non-trivial real eigenvalues, the vortex is stable.

In the next subsection, we shall demonstrate that mesoscale vortices with uniform PV in the lower layer fall into the last category.

4.3. Vortices with uniform PV in the lower layer

Consider the eigenvalue problems (23) and (24) for LLD-modes and assume

$$\frac{d}{dr}\left[\frac{1}{r}\frac{d}{dr}(rV_2)\right] + V_1 = 0 \tag{33}$$

(which is what the condition of uniform lower-layer PV amounts to in the leading order). Then, (23) yields:

$$\frac{1}{r}\frac{d}{dr}\left(r\frac{d\phi_2^{(0)}}{dr}\right) - \frac{k^2}{r^2}\phi_2^{(0)} = 0.$$

One can readily see that this equation has no bounded solutions.

Next, to prove the stability of M-modes, substitute (33) into the M-mode equation (31) and rewrite it in the form:

$$\frac{d}{dr}\left[\frac{1}{r}\frac{d}{dr}(r\phi_2^{(1)})\right] + V_1 = 0.$$

Comparing this equation with (33), one can deduce that

$$\phi_2^{(1)} = V_2 + Ar + \frac{B}{r}. \tag{34}$$

To satisfy the boundary conditions (30), put

$$A = 0, \qquad B = 0. \tag{35}$$

---

[3] In principle, these corrections can be examined through an asymptotic approach used for similar problems by Schecter et al. (2001), Balmforth et al. (2001), Schecter and Montgomery (2003) and Benilov (2003).

Finally, we substitute (34) and (35) into (32) and obtain:

$$c^{(1)} \int_0^\infty r^2 V_1 \, \mathrm{d}r = 0. \tag{36}$$

Since the net upper-layer angular momentum is non-zero [see (4)], it follows from (36) that $c^{(1)} = 0$, which is, in fact, the trivial solution (18) and should be discarded.

Thus, for monopolar vortices with uniform PV in the lower layer, the M-problem admits only the trivial solution, and the LLD-problem does not admit any solutions at all. We conclude that vortices with uniform PV are baroclinically stable.

As for ULD-modes, these are not sensitive to deep flow [observe that V_2 does not appear in equation (21)]; hence, the barotropic stability of a vortex is determined by its profile in the upper layer. We shall not discuss ULD-modes in more detail, as barotropic effects play no part in the instability of mesoscale rings (recall that, out of the three vortex profiles considered, only the Gaussian profile was barotropically unstable and, even in this case, none of the 'real' rings fell into the region of barotropic instability; see Figs. 2a and 4a).

5. Concluding remarks

Thus, we have examined two-layer vortices with uniform PV in the lower layer, with respect to linear harmonic disturbances (normal modes). Both numerical and asymptotic studies showed that such vortices are stable, providing a model, which consistently describes the observed lifespans of oceanic rings.

It should be emphasized that, everywhere in this work, the upper layer of the ocean was assumed thin $(\varepsilon = H_1/H_2 \ll 1)$. Given this assumption, the *strong* effect of a *weak* deep flow should not come as a surprise: after all, the lower layer is thick, and its net characteristics (e.g. angular momentum) can be comparable to, or even exceed, those in the upper layer.

Appendix A. Properties of the eigenvalue problems (25)–(30)

First, we shall prove that the leading-order problems (25) and (26) have a solution only for the first azimuthal wavenumber,

$$k = 1. \tag{A.1}$$

Indeed, introduce χ such that

$$\phi_1^{(0)} = V_1 \chi \tag{A.2}$$

and rewrite (25) and (26) in the form:

$$\frac{\mathrm{d}}{\mathrm{d}r}\left(rV_1^2 \frac{\mathrm{d}\chi}{\mathrm{d}r}\right) - \frac{k^2-1}{r}V_1^2 \chi = 0, \tag{A.3}$$

$$V_1 \chi \to 0 \quad \text{as} \quad r \to 0, \infty. \tag{A.4}$$

Multiply (A.3) by χ^* and integrate over $0 < r < \infty$. Integrating by parts (twice) and using (A.4), we obtain:

$$\int_0^\infty V_1^2 \left(r \left| \frac{d\chi}{dr} \right|^2 + \frac{k^2 - 1}{r} |\chi|^2 \right) dr = 0.$$

Clearly, if $k \neq 1$, then,

$$\frac{d\chi}{dr} = 0, \qquad \chi = 0, \quad \text{at all points where } V_1 \neq 0,$$

which makes χ zero everywhere (if a solution and its derivative of a second-order ODE with continuous coefficients are both zero at the same point, this solution is zero identically). If, however, $k = 1$, the solution evidently exists: $\chi = \text{const}$. Putting const $= 1$ and recalling (A.2), we obtain:

$$\phi_1^{(0)} = V_1. \tag{A.5}$$

Now, substitution of (A.1) and (A.5) into the lower-layer equation (29) yields (31).

Finally, we shall eliminate $\phi_1^{(1)}$ by integrating (27) over $0 < r < \infty$. Integrating by parts (twice), using the boundary conditions (28), and taking into account (A.5), we obtain equation (32).

References

Balmforth, N.J., Llewellyn Smith, S.G., Young, W.R., 2001. Disturbing vortices. J. Fluid Mech. 426, 95–133.

Benilov, E.S., 2003. Instability of quasigeostrophic vortices in a two-layer ocean with thin upper layer. J. Fluid Mech. 475, 303–331.

Benilov, E.S., 2004. Stability of vortices in a two-layer ocean with uniform potential vorticity in the lower layer. J. Fluid Mech. 502, 207–232.

Benilov, E.S., Broutman, D., Kuznetsova, E.P., 1998. On the stability of large-amplitude vortices in a continuously stratified fluid on the *f*-plane. J. Fluid Mech. 355, 139–162.

Carton, X.J., McWilliams, J.C., 1989. Barotropic and baroclinic instabilities of axisymmetric vortices in a quasi-geostrophic model. In: Nihoul, J.C.J., Jamart, B.M. (Eds.), Mesoscale/Synoptic Coherent Structures in Geophysical Turbulence. Elsevier Oceanography Series, vol. 50. Elsevier, Amsterdam, pp. 225–244.

Carton, X.J., McWilliams, J.C., 1996. Nonlinear oscillatory evolution of a baroclinically unstable geostrophicvortex. Dyn. Atmos. Oceans 24, 207–214.

Dewar, W.K., Killworth, P.D., 1995. On the stability of oceanic rings. J. Phys. Oceanogr. 25, 1467–1487.

Flierl, G.R., 1988. On the instability of geostrophic vortices. J. Fluid Mech. 197, 349–388.

Helfrich, K.R., Send, U., 1988. Finite-amplitude evolution of two-layer geostrophic vortices. J. Fluid Mech. 197, 331–348.

Ikeda, M., 1981. Instability and splitting of mesoscale rings using a two-layer quasi-geostrophic model on an *f*-plane. J. Phys. Oceanogr. 11, 987–998.

Katsman, C.A., Van der Vaart, P.C.F., Dijkstra, H.A., de Ruijter, W.P.M., 2003. On the stability of multi-layer ocean vortices: a parameter study including realistic Gulf Stream and Agulhas rings. J. Phys. Oceanogr. 33, 1197–1218.

Killworth, P.D., Blundell, J.R., Dewar, W.K., 1997. Primitive equation instability of wide oceanic rings. Part 1. Linear theory. J. Phys. Oceanogr. 27, 941–962.

Lai, D.Y., Richardson, P.L., 1977. Distribution and movement of Gulf Stream rings. J. Phys. Oceanogr. 7, 670–683.

Olson, D.B., 1991. Rings in the ocean. Ann. Rev. Earth Planet. Sci. 19, 283–311.

Sokolovskiy, M.A., 1988. Numerical modelling of nonlinear instability for axisymmetric two-layer vortices. Izv. Atmos. Ocean. Phys. 24, 735–743.

Sokolovskiy, M.A., 1997. Stability of axisymmetric three-layer vortices. Izv. Atmos. Ocean. Phys. 33, 19–30.

Paldor, N., Nof, D., 1990. Linear instability of an anticyclonic vortex in a two-layer ocean. J. Geophys. Res. 95, 18075–18079.

Schecter, D.A., Montgomery, M.T., 2003. On the symmetrization rate of an intense geophysical vortex. Dyn. Atmos. Oceans 37, 55–88.

Schecter, D.A., Montgomery, M.T., Reasor, P.D., 2001. A theory for the vertical alignment of a quasigeostrophic vortex. J. Atmos. Sci. 59, 150–168.